

NNLO corrections to Z+H production at lepton colliders

Ayres Freitas^{a,*} and Qian Song^b

^a*Pittsburgh Particle-physics Astro-physics & Cosmology Center(PITT-PACC), Department of Physics & Astronomy, University of Pittsburgh, Pittsburgh, PA 15260, USA*

^b*Department of Physics and Astronomy, Ghent University, 9000 Ghent, Belgium*

E-mail: afreitas@pitt.edu, qian.song@ugent.be

A technique for computing electroweak next-to-next-to-leading order (NNLO) corrections with arbitrary masses is described. It is based on using a dispersion relation and Feynman parameters for one of the two subloops and leads to low-dimensional numerical integrals for any $2 \rightarrow 2$ scattering process. UV divergencies can be treated with suitable subtraction terms. As a concrete phenomenological application, the calculation of electroweak NNLO corrections with closed fermion loops to the process $e^+e^- \rightarrow ZH$ is discussed.

*Loops and Legs in Quantum Field Theory (LL2024)
14-19, April, 2024
Wittenberg, Germany*

*Speaker

1. Introduction

Higher-order radiative corrections are becoming increasingly relevant for the the physics program at the (HL-)LHC and for future e^+e^- Higgs factories, such as ILC [1, 2], FCC-ee [3] and CEPC [4]. However, their calculation at 2-loop order and beyond poses challenges due to the presence of many massive propagators with different mass scales (m_W, m_Z, m_H, m_t) in the loops.

Analytical techniques, which have been successfully applied to many NNLO and NNNLO QCD contribution for LHC production processes (see Ref. [5] for a recent review), require two important steps: (i) a reduction to master integrals using integration-by-parts (IBP) relations; and (ii) analytical solutions of the master integrals themselves. For problems with many mass scales, step (i) becomes computationally very expensive and intermediate expressions may become uncontrollably large. For step (ii), the currently known function space (generalized harmonic polylogarithms, iterated elliptic integrals) may not be sufficient to describe all MIs that appear in calculations with many massive propagators. This last issue can be circumvented by recent developments in solving differential equations for the MIs using generalized power series expansions [6–10], but the IBP reduction is still needed for these approaches.

On the hand, direct numerical integration methods can in principle be used without IBP reduction. The numerical integration could be implemented for different variable choices (e.g. in momentum space, Feynman parameter space, etc.), but in all cases one obtains multi-dimensional numerical integrals that have to be evaluation with (quasi-)Monte-Carlo integration and that converge relatively slowly. See Ref. [5] for more details.

This work presents a semi-numerical technique that is tailored for electroweak 2-loop corrections and more efficient for such problems than the more general approaches. This techniques has previously been introduced in Refs. [11, 12] As a concrete application, the results for fermionic electroweak NNLO corrections to $e^+e^- \rightarrow ZH$ will be presented [12, 13].

2. Computational approach

Let us first consider 2-loop integrals with a sub-loop self-energy bubble. As proposed in Ref. [14], for integrals with trivial numerators, the sub-loop bubble can be expressed as a dispersion integral,

$$B_0(p^2, m_1^2, m_2^2) = \int_{(m_1+m_2)^2}^{\infty} d\sigma \frac{\Delta B_0(\sigma, m_1^2, m_2^2)}{\sigma - p^2 - i\epsilon}, \quad (1)$$

where D is the space-time dimension and $\Delta B_0(\sigma, m_1^2, m_2^2) \equiv \frac{1}{\pi} \text{Im} B_0(\sigma, m_1^2, m_2^2)$ is the discontinuity of the one-loop scalar two-point function B_0 across the branch cut, which lies along the positive real axis in the complex p^2 plane (see Fig. 2 left). When inserting (1) into a two-loop integral, it provides one more propagator for the outer loop momentum p with mass σ . Thus the d^4p integral can be expressed in terms of well-known analytical one-loop functions (see e.g. Ref. [15, 16]):

$$I^{2\text{-loop}} = - \int d\sigma \Delta B_0(\sigma, \dots) I^{1\text{-loop}}(\dots, \sigma). \quad (2)$$

For a complete Feynman diagram, with non-trivial terms in the numerator, the self-energy sub-loop contains higher-rank Passarino-Veltman (PV) functions, (B_1, B_{00} , etc.), for which one a dispersion

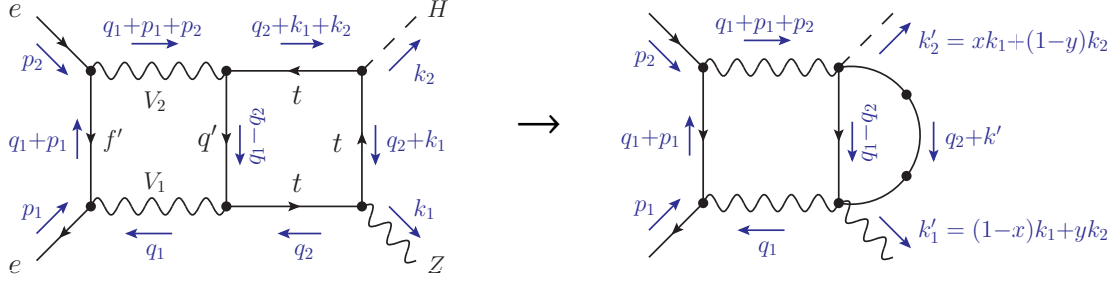


Figure 1: Planar two-loop box diagrams with top quarks in the loop (left), and illustration of the effect of introducing Feynman parameters for the q_2 propagators (right).

relation can be derived analogously. Similarly, the second loop integral in general contains higher-rank (PV) functions in $I^{1-\text{loop}}$.

To apply this idea to diagrams with sub-loop triangles and boxes, Feynman parameters are introduced. For example, in the diagram in Fig. 1, three of the top-quark propagators can be combined with the help of two Feynman parameters. As a result, the q_2 sub-loop is transformed to the topology of a self-energy bubble, and thus one can introduce a dispersion relation of the form

$$q_2 \text{ loop} = \int dx dy \frac{\partial^2}{\partial (m'^2)^2} \int_{\sigma_0}^{\infty} d\sigma \frac{\Delta B_0(\sigma, m'^2, m_{q'}^2)}{\sigma - \tilde{q}_1^2}, \quad (3)$$

$$\tilde{q}_1 = q_1 + k' + i\epsilon, \quad k' = (1-x)k_1 + yk_2,$$

$$m'^2 = m_t^2 - xy(k_1 + k_2)^2 - (1-x-y)(xk_1^2 + yk_2^2), \quad \sigma_0 = (m' + m_{q'})^2.$$

The derivative with respect to m'^2 can be pulled inside the σ integral:

$$q_2 \text{ loop} = \int dx dy \left\{ \int_{\sigma_0}^{\infty} d\sigma \frac{\partial_{m'}^2 \Delta B_0(\sigma, m'^2, m_{q'}^2)}{\sigma - \tilde{q}_1^2} - \left[\frac{\partial_{m'} \Delta B_0(\sigma, m'^2, m_{q'}^2)}{\sigma - \tilde{q}_1^2} \right]_{\sigma \rightarrow \sigma_0} \right\}, \quad (4)$$

where $\partial_{m'} \equiv \frac{\partial}{\partial (m'^2)}$. The derivatives of the ΔB_0 function can be easily computed, but a problem occurs since the two terms in (4) are individually divergent for $\sigma \rightarrow \sigma_0$. This can be fixed by modifying the integrand such that the boundary terms are cancelled, viz.

$$q_2 \text{ loop} = \int dx dy \left\{ \int_{\sigma_0}^{\infty} d\sigma \partial_{m'}^2 \Delta B_0(\sigma, m'^2, m_{q'}^2) \left(\frac{1}{\sigma - \tilde{q}_1^2} - \frac{\sigma_0}{\sigma(\sigma_0 - \tilde{q}_1^2)} \right) + \frac{\sigma_0}{\sigma_0 - \tilde{q}_1^2} \partial_{m'}^2 B_0(0, m'^2, m_{q'}^2) \right\}. \quad (5)$$

where the extra term in the integrand is added back in integrated form.

A second difficulty arises from the fact the m'^2 can become negative, so that the branch point of the B_0 function moves into the complex plane, and the dispersion relation (1) cannot be used anymore. It is, however, possible to choose a different complex integration contour, which yields a modified dispersion relation, as illustrated in Fig. 2 (right). The new dispersion relation kernel involves the B_0 function itself rather than its discontinuity. This construction extends to higher-rank PV functions B_1, B_{00}, \dots , as mentioned above.

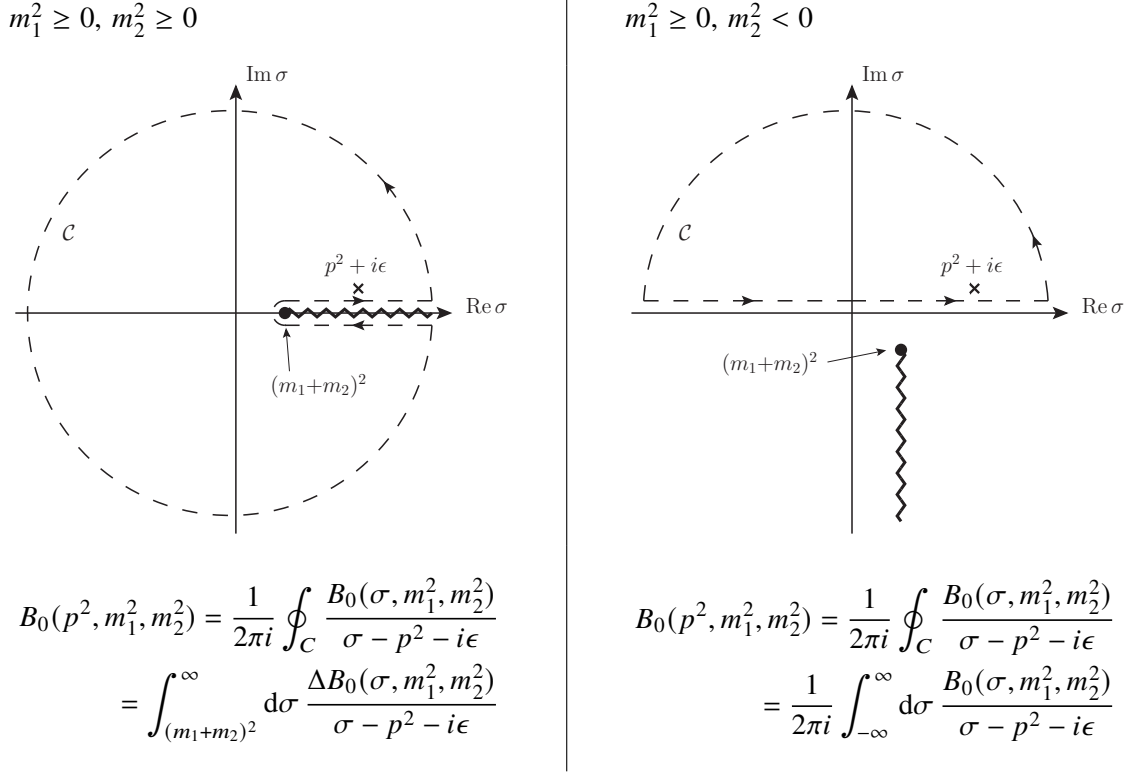


Figure 2: Contours for the dispersion relations for the one-loop scalar self-energy function B_0 for the cases $m_1^2, m_2^2 > 0$ (left) and $m_1^2 < 0, m_2^2 > 0$ (right). The zigzag lines denote the branch cuts. The circle sections are understood to have a radius $R \rightarrow \infty$ and a vanishing contribution to the contour integrals.

By following the above steps, 2-loop box diagrams can be transformed into three-dimensional numerical integrals (with integration variables x, y, σ) that can be reliably evaluated using adaptive Gauss integration or similar integration algorithms. Vertex diagrams can be similarly constructed, and they typically only require one Feynman parameter.

3. UV divergences

In general, 2-loop integrals can be UV divergent, which will cause the numerical σ -integral to diverge. Thus one needs to introduce suitable subtraction terms to make the integral finite. The subtraction terms should be simple enough to integrate analytically and add back to the whole expression. At the 2-loop level, integrals can have global (nested) divergences and sub-loop divergences. To illustrate the construction of subtraction terms, let us consider the following concrete example:

$$\mathcal{I} = \int_{q_1} \int_{q_2} \frac{1}{(q_2^2 - m_{V_2}^2)((q_2 + p)^2 - m_{V_1}^2)((q_2 + q_1)^2 - m_{f_1}^2)} \times \frac{q_1^4}{(q_1^2 - m_{f_2}^2)((q_1 - p_h)^2 - m_{f_2}^2)((q_1 - p)^2 - m_{f_2}^2)}, \quad (6)$$

where for the sake of brevity we have not spelled out the $q_{1,2}$ integration measures.

The global divergence correspond to the limit $q_{1,2} \rightarrow \infty$, and therefore a suitable subtraction terms in obtained by setting the external momenta to zero:

$$\mathcal{I}_{\text{sub}}^{\text{glob}} = \int_{q_1} \int_{q_2} \frac{q_1^4}{(q_2^2 - m_{V_2}^2)(q_2^2 - m_{V_1}^2)((q_2 + q_1)^2 - m_{f_1}^2)(q_1^2 - m_{f_2}^2)^3}. \quad (7)$$

This term can be evaluated in terms of 2-loop vacuum integrals, for which analytical expressions are known. In our case, this step has been carried out with the help of FIRE 5 [17] and TVID [18].

The sub-loop divergences correspond to the taking the limit of only $q_1 \rightarrow \infty$ or $q_2 \rightarrow \infty$. For the q_1 sub-loop divergence, a subtraction term can thus be constructed by neglecting all other momenta in the q_1 -dependent propagators:

$$\begin{aligned} \mathcal{I}_{\text{sub}}^{q_1} &= \int_{q_1} \int_{q_2} \frac{1}{(q_2^2 - m_{V_2}^2)((q_2 + p)^2 - m_{V_1}^2)} \times \frac{q_1^4}{(q_1^2 - m_{f_1}^2)(q_1^2 - m_{f_2}^2)^3} \\ &= B_0(p^2, m_{V_1}^2, m_{V_2}^2) \times [c_1 A_0(m_{f_1}^2) + c_2 A_0(m_{f_2}^2)]. \end{aligned} \quad (8)$$

$\mathcal{I}_{\text{sub}}^{q_1}$ factorizes into two terms that depend only on q_1 and q_2 , respectively, and so they can straightforwardly be evaluated in terms of well-known basic one-loop functions. Here $c_{1,2}$ are coefficients that depend on $m_{f_{1,2}}$ and D , which we do not spell out for the sake of brevity.

Similarly, the q_2 sub-loop divergence will lead to a factorized integral. Thus in total one obtains

$$\mathcal{I} = \underbrace{[\mathcal{I} - \mathcal{I}_{\text{sub}}^{\text{glob}} - \mathcal{I}_{\text{sub}}^{q_1} - \mathcal{I}_{\text{sub}}^{q_2}]}_{\text{integrate numerically}} + \underbrace{[\mathcal{I}_{\text{sub}}^{\text{glob}} + \mathcal{I}_{\text{sub}}^{q_1} + \mathcal{I}_{\text{sub}}^{q_2}]}_{\text{integrate analytically}}. \quad (9)$$

Here the first term on the right-hand side is UV-finite and can be numerically evaluated using the techniques described in the previous section. The remaining terms can be computed analytically in terms of known basic integrals, and they account for the UV divergences that eventually cancel when performing the renormalization.

4. Fermionic electroweak NNLO corrections to $e^+e^- \rightarrow ZH$

In Refs. [12, 13], the approach described above has been applied to the calculation of electroweak NNLO corrections with closed fermion loops (henceforth called ‘‘fermionic EW NNLO corrections’’) to the process $e^+e^- \rightarrow ZH$. This is the main Higgs-boson production process at future e^+e^- Higgs factories, and its cross-section can be measured with sub-percent precision at FCC-ee and CEPC [3, 4]. Previously, NLO [19–21] and mixed EW-QCD NNLO [22, 23] corrections to this process have been computed, but the uncertainty from missing EW NNLO corrections has been estimate to be or $O(1\%)$, and thus it is necessary to take them into account. For an alternative approach to computing these corrections, see Ref. [24].

For the practical implementation of our calculation, diagrams and matrix elements have been generated with FeynArts 3.11 [25], and additional algebraic manipulations were performed in Mathematica¹, such as

¹FeynCalc 9 [26] was used for some steps, with cross-checks against an in-house code.

- the construction of the integrand for the numerical integration (including the introduction of Feynman parameters and dispersion relations) for each diagram type;
- introduction of UV subtraction term;
- generation of C++ code for the subtracted integrand.

As mentioned above, no IBP reduction was performed, but instead the integrand is expressed in terms of higher-rank PV functions. For the numerical evaluation of these functions `LoopTools 2.16` [27] has been used. The numerical integration has been implemented using adaptive Gauss quadrature algorithms from the `Boost` library [28] and the `Quadpack` library [29].

To improve the numerical stability, the upper limit ∞ of the σ integrals has been replaced by a finite cutoff, and a small explicit imaginary part has been introduced for negative squared masses to ensure that `LoopTools` picks the correct complex branch. It has been checked that the dependence on variations of the cutoff (by a factor 2 up or down) and the imaginary part of the masses (by an order of magnitude) is negligible compared to the integration uncertainties. The overall precision is limited by the use of floating point numbers. For double precision numerics, about 3 digits precision of the integrated results can be achieved. This typically requires a few minutes on a single CPU core for one diagram type. In some cases, quadruple precision numerics have been used for additional precision (typically more than 6 digits).

QED radiation in the initial state factorizes from the remaining EW corrections. They contain large logarithm which can be summed to higher orders using the structure function approach [30]. Therefore, to avoid double counting, the virtual initial-state QED corrections are omitted in our calculation. UV divergences have been regularized using dimensional regularization. However, for diagrams that depend on the treatment of γ_5 , any Dirac trace contributions that can lead to Levi-Civita tensors have been computed using 4-dimension algebra, since these contributions are UV-finite at the perturbative order of our calculation. The remaining terms have been computed using D -dimensional algebra with a naively anticommuting γ_5 .

For the renormalization, the on-shell (OS) scheme according to Ref. [31, 32] has been employed. It uses the electromagnetic coupling in the Thomson limit and particle masses as input quantities. We also present results in an alternative scheme, where the electromagnetic coupling has been replaced by the Fermi coupling, G_μ . CKM mixing and the masses of all fermions except the top quark have been neglected in our calculation.

It should be noted that the OS scheme employed here defines the W- and Z-boson masses via the complex pole of the propagator. As a result, the numerical input values for the masses need to be translated according to

$$m_Z = m_Z^{\text{exp}} [1 + (\Gamma_Z^{\text{exp}}/m_Z^{\text{exp}})^2]^{-1/2}, \quad \Gamma_Z = \Gamma_Z^{\text{exp}} [1 + (\Gamma_Z^{\text{exp}}/m_Z^{\text{exp}})^2]^{-1/2}, \quad (10)$$

where the quantities with superscript “exp” indicate the values reported in experimental studies, whereas the quantities without superscript refer to the renormalized parameters in our calculation.

Since the Z boson is unstable, the process $e^+e^- \rightarrow ZH$ is defined via the residue of the leading term in an expansion about the Z pole in the full process $e^+e^- \rightarrow f\bar{f}H$. For the leading pole term, production and decay of the Z boson factorize, and thus it makes sense to talk about a ZH production cross-section. See Ref. [12] for more details.

| | (fb) | Contribution | (fb) |
|------------------------|---------|---------------------------------|---------|
| σ^{LO} | 222.958 | | |
| σ^{NLO} | 229.893 | $\mathcal{O}(\alpha_{N_f=1})$ | 21.130 |
| | | $\mathcal{O}(\alpha_{N_f=0})$ | -14.195 |
| σ^{NNLO} | 231.546 | $\mathcal{O}(\alpha_{N_f=2}^2)$ | 1.881 |
| | | $\mathcal{O}(\alpha_{N_f=1}^2)$ | -0.226 |

Table 1: Numerical results for the integrated cross section for $e^+e^- \rightarrow ZH$ at different electroweak perturbative orders, and also individually showing contributions with different number of closed fermion loops, as indicated by N_f .

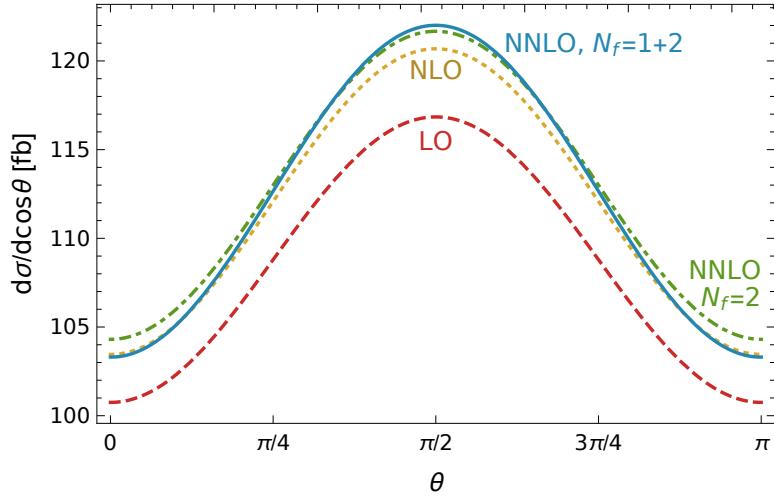


Figure 3: Differential unpolarized cross section for $e^+e^- \rightarrow ZH$ as a function of the scattering angle θ for $\sqrt{s} = 240$ GeV, at different perturbative orders.

With the input parameters

$$\begin{aligned}
 m_W^{\text{exp}} = 80.379 \text{ GeV} &\Rightarrow m_W = 80.352 \text{ GeV}, & m_H = 125.1 \text{ GeV}, & m_t = 172.76 \text{ GeV}, \\
 m_Z^{\text{exp}} = 91.1876 \text{ GeV} &\Rightarrow m_Z = 91.1535 \text{ GeV}, & \alpha^{-1} = 137.036, & \Delta\alpha = 0.059, \\
 \sqrt{s} = 240 \text{ GeV}, & & &
 \end{aligned}
 \tag{11}$$

the results in Tab. 1 and Fig. 3 are obtained. While the correction to the total cross-section from the $\alpha_{N_f=1}^2$ contributions is relatively small, one can see from the figure that there are sizeable corrections to the differential cross-section for different values of the scattering angle θ .

Table 2 shows the corrections to the total cross-section in the $\alpha(0)$ scheme, where the electroweak couplings are parametrized in terms of the electromagnetic coupling at zero momentum transfer, and the G_μ scheme, where the electroweak couplings are parametrized in terms of the Fermi constant. The translation between the two schemes is given by $\frac{G_\mu}{\sqrt{2}} = \frac{\pi\alpha}{2m_W^2(1-m_W^2/m_Z^2)}(1+\Delta r)$, where Δr accounts for radiative corrections, for which we use the results from Refs. [32, 33].

| | $\alpha(0)$ scheme | G_μ scheme |
|--|--------------------|----------------|
| σ^{LO} [fb] | 223.14 | 239.64 |
| σ^{NLO} [fb] | 229.78 | 232.46 |
| $\sigma^{\text{NNLO,EW}\times\text{QCD}}$ [fb] | 232.21 | 233.29 |
| $\sigma^{\text{NNLO,EW}}$ [fb] | 233.86 | 233.98 |

Table 2: Results for the total cross-section for $e^+e^- \rightarrow ZH$, using input values and mixed EW-QCD corrections from Ref. [23].

As evident from Tab. 2, the predictions in the two schemes are in very good agreement, but the order-by-order corrections are smaller in the G_μ scheme.

5. Summary

This contribution describes a new semi-numerical technique for general 2-loop calculations with arbitrary massive propagators. It makes use of dispersion relations and Feynman parameters. Since it avoids integration-by-parts reduction and numerical integrals of high dimensionality, it is relative efficient and requires modest computational resources. The numerical precision of the method is limited by the machine floating point numbers, but it is sufficient for practical phenomenological applications.

One such application are the fermionic electroweak NNLO corrections to the process $e^+e^- \rightarrow ZH$. The corrections were found to be modest in size, but not negligible for the purposes of future e^+e^- Higgs factories. The dependence on the renormalization scheme is significantly reduced by including the electroweak NNLO corrections. Judging by the remaining scheme dependence, as well as parametric power-counting estimates, the missing bosonic electroweak NNLO corrections are expected to be numerically less important, but their computation would still be useful and in general achievable with the methods described here.

Acknowledgments

This work has been supported in part by the National Science Foundation under grant no. PHY-2112829.

References

[1] H. Baer *et al.* *The International Linear Collider Technical Design Report - Volume 2: Physics*, [arXiv:1306.6352 [hep-ph]].

[2] P. Bambade *et al.* *The International Linear Collider: A Global Project*, [arXiv:1903.01629 [hep-ex]].

[3] A. Abada *et al.* [FCC Collaboration], *FCC-ee: The Lepton Collider : Future Circular Collider Conceptual Design Report Volume 2*, Eur. Phys. J. ST **228**, 261 (2019).

- [4] J. B. Guimarães da Costa *et al.* [CEPC Study Group], *CEPC Conceptual Design Report: Volume 2 – Physics & Detector*, arXiv:1811.10545 [hep-ex].
- [5] G. Heinrich, *Collider Physics at the Precision Frontier*, Phys. Rept. **922**, 1-69 (2021) [arXiv:2009.00516 [hep-ph]].
- [6] X. Liu, Y. Q. Ma and C. Y. Wang, *A Systematic and Efficient Method to Compute Multi-loop Master Integrals*, Phys. Lett. B **779**, 353-357 (2018) [arXiv:1711.09572 [hep-ph]].
- [7] F. Moriello, *Generalised power series expansions for the elliptic planar families of Higgs + jet production at two loops*, JHEP **01**, 150 (2020) [arXiv:1907.13234 [hep-ph]].
- [8] M. Hidding, *DiffExp, a Mathematica package for computing Feynman integrals in terms of one-dimensional series expansions*, Comput. Phys. Commun. **269**, 108125 (2021) [arXiv:2006.05510 [hep-ph]].
- [9] X. Liu and Y. Q. Ma, *AMFlow: A Mathematica package for Feynman integrals computation via auxiliary mass flow*, Comput. Phys. Commun. **283**, 108565 (2023) [arXiv:2201.11669 [hep-ph]].
- [10] T. Armadillo, R. Bonciani, S. Devoto, N. Rana and A. Vicini, *Evaluation of Feynman integrals with arbitrary complex masses via series expansions*, Comput. Phys. Commun. **282**, 108545 (2023) [arXiv:2205.03345 [hep-ph]].
- [11] Q. Song and A. Freitas, *On the evaluation of two-loop electroweak box diagrams for $e^+e^- \rightarrow HZ$ production*, JHEP **04**, 179 (2021) [arXiv:2101.00308 [hep-ph]].
- [12] A. Freitas and Q. Song, *Two-Loop Electroweak Corrections with Fermion Loops to $e + e^- \rightarrow ZH$* , Phys. Rev. Lett. **130**, 031801 (2023) [arXiv:2209.07612 [hep-ph]].
- [13] A. Freitas, Q. Song and K. Xie, *Fermionic electroweak NNLO corrections to $e + e^- \rightarrow ZH$ with polarized beams and different renormalization schemes*, Phys. Rev. D **108**, 053006 (2023) [arXiv:2305.16547 [hep-ph]].
- [14] S. Bauberger, F. A. Berends, M. Bohm and M. Buza, Nucl. Phys. B **434**, 383-407 (1995) [arXiv:hep-ph/9409388 [hep-ph]].
- [15] G. 't Hooft and M. J. G. Veltman, *Scalar One Loop Integrals*, Nucl. Phys. B **153**, 365-401 (1979).
- [16] G. J. van Oldenborgh and J. A. M. Vermaseren, *New Algorithms for One Loop Integrals*, Z. Phys. C **46**, 425-438 (1990).
- [17] A. V. Smirnov, *FIRE5: a C++ implementation of Feynman Integral REDuction*, Comput. Phys. Commun. **189**, 182-191 (2015) [arXiv:1408.2372 [hep-ph]].
- [18] S. Bauberger, A. Freitas and D. Wiegand, *TVID 2: Evaluation of planar-type three-loop self-energy integrals with arbitrary masses*, JHEP **01**, 024 (2020) [arXiv:1908.09887 [hep-ph]].

- [19] J. Fleischer and F. Jegerlehner, *Radiative Corrections to Higgs Production by $e^+e^- \rightarrow ZH$ in the {Weinberg-Salam} Model*, Nucl. Phys. B **216**, 469 (1983).
- [20] B. A. Kniehl, *Radiative corrections for associated ZH production at future e^+e^- colliders*, Z. Phys. C **55**, 605 (1992).
- [21] A. Denner, J. Küblbeck, R. Mertig and M. Böhm, *Electroweak radiative corrections to $e^+e^- \rightarrow ZH$* , Z. Phys. C **56**, 261 (1992).
- [22] Y. Gong, Z. Li, X. Xu, L. L. Yang and X. Zhao, *Mixed QCD-EW corrections for Higgs boson production at e^+e^- colliders*, Phys. Rev. D **95**, 093003 (2017) [arXiv:1609.03955 [hep-ph]].
- [23] Q. F. Sun, F. Feng, Y. Jia and W. L. Sang, *Mixed electroweak-QCD corrections to $e^+e^- \rightarrow HZ$ at Higgs factories*, Phys. Rev. D **96**, 051301(R) (2017) [arXiv:1609.03995 [hep-ph]].
- [24] X. Chen, X. Guan, C. Q. He, Z. Li, X. Liu and Y. Q. Ma, *Complete two-loop electroweak corrections to $e^+e^- \rightarrow HZ$* , [arXiv:2209.14953 [hep-ph]].
- [25] T. Hahn, *Generating Feynman diagrams and amplitudes with FeynArts 3*, Comput. Phys. Commun. **140**, 418 (2001).
- [26] V. Shtabovenko, R. Mertig and F. Orellana, *New Developments in FeynCalc 9.0*, Comput. Phys. Commun. **207**, 432 (2016) [arXiv:1601.01167 [hep-ph]].
- [27] T. Hahn and M. Perez-Victoria, *Automatized one loop calculations in four-dimensions and D-dimensions*, Comput. Phys. Commun. **118**, 153 (1999), www.feynarts.de/looptools.
- [28] N. Agrawal *et al.*, *Boost Math Toolkit 2.13.0*, www.boost.org/doc/libs/master/libs/math/doc/html/index.html.
- [29] R. Piessens, E. de Doncker-Kapenga, C. W. Überhuber, D. K. Kahanger, *QUADPACK, A Subroutine Package for Automatic Integration*, Springer, Berlin (1983).
- [30] M. Greco, G. Montagna, O. Nicrosini, F. Piccinini and G. Volpi, *ISR corrections to associated HZ production at future Higgs factories*, Phys. Lett. B **777**, 294-297 (2018). [arXiv:1711.00826 [hep-ph]].
- [31] A. Denner, *Techniques for calculation of electroweak radiative corrections at the one loop level and results for W physics at LEP-200*, Fortsch. Phys. **41**, 307-420 (1993) [arXiv:0709.1075 [hep-ph]].
- [32] A. Freitas, W. Hollik, W. Walter and G. Weiglein, *Electroweak two loop corrections to the $M_W - M_Z$ mass correlation in the standard model*, Nucl. Phys. B **632**, 189-218 (2002) [erratum: Nucl. Phys. B **666**, 305-307 (2003)] [arXiv:hep-ph/0202131 [hep-ph]].
- [33] A. Freitas, W. Hollik, W. Walter and G. Weiglein, *Complete fermionic two loop results for the $M_W - M_Z$ interdependence*, Phys. Lett. B **495**, 338-346 (2000) [erratum: Phys. Lett. B **570**, 265 (2003)] [arXiv:hep-ph/0007091 [hep-ph]].